SEMICONDUCTOR THERMOELASTIC SOLID SPHERE UNDER MOISTURE AND THERMAL DIFFUSIVITY

Dedicated to Dr. Dan Tiba on the occasion of his 70th anniversary

Eduard-Marius CRACIUN[1], Iqbal KAUR[2], Kulvinder SINGH[3]

Abstract. This paper has introduced a novel approach to simulate the thermal and moisture diffusivity in a semiconducting solid sphere, based on two-temperature theory of thermoelasticity. By incorporating two-temperature theory, it accounts for the interplay between the temperature and stress, providing a more accurate representation of the system's behavior. The research focuses on the behavior of the sphere when it is subjected to a laser pulse that induces varying heat flux on its boundary surface. By utilizing the Laplace transform technique, the mathematical model is solved in the transformed domain to meet the intended objective. The mathematical model is numerically inverted to obtain a comprehensive understanding of the physical parameters in the physical domain. A graphic representation of various parameters under the effect of moisture diffusivity at two different temperatures are generated using the MATLAB software. The model offers a comprehensive approach to accurately represent thermal and moisture diffusivities of the solid sphere, enabling a deeper comprehension of the various phenomena observed in a wide range of the semiconductor devices. By utilizing this model, the engineers and designers can enhance their ability to effectively design these devices, ensuring optimal performance and functionality.

Keywords: Moisture diffusivity, Thermal diffusivity, Semiconducting sphere, Two temperature.

DOI **10.56082/annalsarsciphyschem.2024.1.27**

[1] mcraciun@univ-ovidius.ro Faculty of Mechanical, Industrial and Maritime Engineering, "Ovidius" University of Constanta, 900527 Constanta, Romania; Academy of Romanian Scientists, IIfov Street, Bucharest, Romania
[2] bawahanda@gmail.com Faculty of Mathematics, Government College for Girls, Palwal, Kurukshetra - 136118, India
[3] ksingh2015@kuk.ac.in Faculty of Engineering, UIET, Kurukshetra University Kurukshetra - 136118, Haryana, India

Nomenclature

δ_{ij}	Kronecker delta,	β_{ij}	Thermal elastic coupling tensor,
e_{ij}	Strain tensors(mm^{-1}),	u_i	Components of displacement(m),
D_m	Moisture diffusivity coefficient,	a_{ij}	Two temperature parameter,
D_E	Carrier diffusion coefficients,	e_{kk}	Cubical dilatation,
K_{ij}	Coefficient of Thermal conductivity,	ρ	Medium density (Kgm^{-3}),
ϵ_{ijk}	Permutation symbol,	D_T^m, D_m^T	Cross-coupled diffusivities
λ, μ	Lame's elastic constants,	φ	Conductive temperature,
D_T	Temperature diffusivity	$\mathcal{K}$	Coupling parameter for thermal activation,
K_{ij}^*	Materialistic constant,	t	Time,
m	Moisture concentration	K_m	Moisture diffusivity
N	Carrier density,	d_n	Coefficient of electronic deformation,
τ_0	Thermal relaxation parameter,	N_0	Carrier concentration atequilibrium position
δ_n	Electronic deformation coefficient,	D_E	Carrier diffusion coefficient
α_t	Linear thermal expansion coefficient,	σ_{ij}	Stress tensors(Nm^{-2}),
s_v	surface recombination velocity	C_E	Specific heat at constant strain,
c	Heat capacity	τ	Photo-generated carrier lifetime,
m_0	Two temperatures,	T_0	Reference temperature s.t. $\lvert T/T_0 \rvert << 1$
T	Thermodynamic temperature,	E_g	Energy gap of the semiconductorparameter.

1. Introduction

The hygro-thermoelastic behavior of a solid semiconductor sphere with two temperature is a complex phenomenon that involves the interaction of moisture, heat, and mechanical stress within the material. This type of analysis is crucial in understanding the performance and reliability of semiconductor devices, which are used in a wide range of technological applications, including electronics, solar cells, and optoelectronics. The behavior of such semiconductors under different environmental conditions, such as varying temperatures and humidity levels, can have a significant impact on their functionality and durability. Understanding the hygro-thermoelastic behavior of solid semiconductor spheres is crucial for the design and optimization of semiconductor devices. By analyzing the effects of temperature, humidity, and mechanical stress on the material, we can develop more reliable and efficient devices that can withstand different operating conditions. Furthermore, this knowledge can help in the development of new materials with improved hygro-thermoelastic properties, leading to advancements in various technological fields.

The study of hygro-thermoelastic behavior in solid spheres under the influence of moisture and thermal diffusivity is an important area of research in materials science and engineering. Such studies aim to understand the behavior and response of materials to coupled effects of temperature, moisture, and mechanical loading. The hygro-thermoelastic behavior of a solid sphere can be influenced by several factors, including the material properties, moisture diffusion, thermal diffusivity, and boundary conditions.

Moisture diffusion is often modeled using Fick's law of diffusion, which describes how moisture moves within the material due to differences in moisture concentration. The

interaction between moisture diffusion and mechanical loading can result in stresses and strains, leading to changes in the mechanical response of the sphere. Thermal diffusivity describes how heat propagates within a material. In the context of hygro-thermoelastic behavior, thermal diffusivity plays a crucial role in determining how heat is transferred and distributed within the solid sphere under the influence of moisture. It influences the rate at which temperature changes occur and interacts with mechanical loading and moisture diffusion. The material properties of the solid sphere, such as elastic modulus, Poisson's ratio, and coefficient of thermal expansion, play a significant role in its hygro-thermoelastic behavior. These properties can vary with moisture content, which affects the mechanical and thermal response of the sphere. Moreover, the boundary conditions applied to the solid sphere can influence its response to hygro-thermoelastic effects. For instance, temperature and moisture gradients at the boundaries can induce stresses and strains within the sphere, leading to deformation or failure.

Understanding the hygro-thermoelastic behavior of solid sphere under the influence of moisture and thermal diffusivity is important for various applications. It can help engineers and researchers design and optimize materials and structures that are subjected to environmental conditions involving moisture and temperature changes, such as composite materials, and electronic devices.

Researchers in the field of nanotechnology have shown a significant interest in semiconductor nanostructures. To fully comprehend semiconducting micro/nanodevices, it is essential to study thermoelasticity. This is because, according to thermoelasticity, semiconducting materials can be classified as elastic materials. Several theoretical models have been explored to understand the relationship between photothermal equations and thermoelasticity. By delving into these models, researchers can gain a better understanding of the behavior of semiconducting materials and their potential applications in nanotechnology. The classical uncoupled thermoelasticity theory, initially proposed by Duhamel [1], presents two notable limitations. Firstly, this theory assumes that the state of elastic materials remains unaffected by temperature variations, disregarding any potential thermal effects on the material's behavior. Secondly, due to the parabolic nature of the heat equation, this theory predicts that temperature propagates at an infinite speed, contradicting experimental evidence and the fundamental principles of physics. These limitations highlight the need for further advancements in thermoelasticity theories to accurately capture the intricate coupling between temperature and elasticity in materials. Coupled thermoelasticity, as proposed by Biot[2], offers a viable solution to the problems at hand. This theory establishes a relationship between the equations of heat conduction and elasticity equations, thereby providing a comprehensive understanding of the interplay between these two phenomena. By considering the effects of thermal expansion and contraction on the mechanical behavior of materials, coupled thermoelasticity enables us to accurately predict the

response of structures to thermal loads. This approach has proven to be particularly useful in the design of high-temperature ap plications, where the effects of thermal stresses can have a significant impact on the performance and durability of materials. The theory in question has a limitation in that it only predicts heat waves that propagate at an unlimited speed.
By utilizing Fourier's law, as suggested by Szekeres [3]-[5], one can effectively express the heat flux in conduction as

$$q^F = -D_T \varphi_{,i}. \tag{1.1}$$

The moisture flux potential can be defined by utilizing Fick's law as:

$$f^F = -D_m m_{,i}. \tag{1.2}$$

Numerous experiments have consistently demonstrated a strong and noteworthy relationship between the movement of moisture and the temperature distribution, and conversely, the temperature field influences the transport of moisture. It has been observed that the existence of moisture concentration gradients leads to the emergence of heat fluxes, which are commonly known as Dufour fluxes. These fluxes can be precisely defined as follows [3]-[5]:

$$q = (q^F + q^D) = -D_T \varphi_{,i} - D_m^T m_{,i}, \tag{1.3}$$

Variations in temperature gradients can potentially influence the moisture flux, also known as the Soret flux

$$f = (f^F + f^S) = -D_m m_{,i} - D_T^m \varphi_{,i}. \tag{1.4}$$

The potential for heat and moisture flux can be determined by analyzing the diffusion of heat and moisture together as

$$q = (q^F + q^D) = -D_T \varphi_{,i} - D_m^T m_{,i}, \tag{1.5}$$

$$f = (f^F + f^S) = -D_m m_{,i} - D_T^m \varphi_{,i}. \tag{1.6}$$

However, when a temperature gradient is suddenly imposed on a homogeneous and isotropic medium, Cattaneo [6] and Vernotte [7, 8] propose a more comprehensive form of Fourier law that takes into account a relaxation time. In the study conducted by Lord and Shulman [9], a comprehensive theory of thermoelasticity was introduced, specifically focusing on an isotropic body with a single relaxation time. This theory

encompasses a hyperbolic heat equation, indicating that the propagation of temperature occurs at a finite speed. The findings of this research shed light on the intricate dynamics of thermoelastic behavior, providing valuable insights into the thermal properties of materials. Green and Lindsay [10] presented a comprehensive analysis of thermoelasticity, offering a more refined comprehension of this field. Their study focused on elucidating the symmetry of the linear heat conduction tensor, providing valuable insights into the behavior of heat transfer in elastic materials. Dhaliwal and Sherief [11] further expanded on this concept by providing comprehensive thermoelasticity equations for an anisotropic medium. These findings have significant implications for the study of heat transfer and material properties, and can be applied in a variety of fields such as engineering and physics. Green and Naghdi [12]-[14] introduced thermoelastic theories that encompass both linear and nonlinear behavior, considering the presence or absence of energy dissipation. They further extended the Fourier law to account for these variations.

The study conducted by Fernandez & Quintanilla [15] delved into the linear thermoelastic deformations of dielectrics. In the scenario where a SM is exposed to an external laser beam, the absorption of optical energy leads to the generation of excited free electrons with a semiconductor gap energy E g, resulting in the formation of a carrier-free charge density. Consequently, both electronic distortion and elastic vibration undergo changes. It is important to note that in this particular situation, the presence of thermal-elastic-plasma waves will have a significant influence on the heat conductivity equations. In their study, Kaur et al. [16] investigated the impact of exponential laser pulse on a semi-conducting solid sphere. They specifically focused on the influence of MGTPT and Hall current effect on the sphere. In addition to these Kaur & Singh [17, 18], Zhang and Li [19], Lata and Kaur [18], Mohamed et al. [20], Kaur et al. [21]-[23], Ebrahimi et al. [24], Lata and Kaur [25], Singh et al. [26] also done studies on the Hall current effect and other theories of thermoelasticity.

In this study, we investigate the hygro-thermoelastic behavior of a solid semiconductor sphere using two temperature model. This model takes into account the coupling between the electronic and lattice temperatures, as well as the effects of moisture diffusion and mechanical deformation. By considering these factors, we can accurately predict the changes in the material's properties, such as thermal expansion, electrical conductivity, and mechanical strength. In conclusion, the hygro-thermoelastic behavior of solid semiconductor spheres with two temperature is a complex phenomenon that requires a comprehensive analysis. By considering the coupling between temperature, moisture diffusion, and mechanical deformation, we can gain valuable insights into the properties and performance of semiconductor materials. This knowledge is essential for the design, optimization, and advancement of semiconductor devices in various technological applications.

2. Basic ecuations

The equations governing the interaction of hygro-photo-thermoelasticity [3]-[5] are given by:

1. Constitutive relations

$$\sigma_{ij} = \left(\lambda u_{k,k} - \beta^T T - \beta^m m - \delta_n N\right)\delta_{ij} + \mu\left(u_{i,j} + u_{j,i}\right) \tag{2.1}$$

$$\beta^T = (3\lambda + 2\mu)\alpha_T \tag{2.2}$$

$$\beta^m = (3\lambda + 2\mu)\alpha_m \tag{2.3}$$

$$\delta_n = (3\lambda + 2\mu)d_n \tag{2.4}$$

$$\varphi - T = \alpha\nabla^2\varphi \tag{2.5}$$

2. Equation of motion

$$\sigma_{ij,j} + F_i = \rho\ddot{u}_i \tag{2.6}$$

3. Plasma diffusion equation

$$\frac{\partial N}{\partial t} = \left(D_E\nabla^2 N - \frac{N}{\tau}\right) + \mathcal{K}T, \tag{2.7}$$

$$\text{where } \mathcal{K} = \frac{T}{\tau}\frac{\partial N_0}{\partial T}. \tag{2.8}$$

4. Moisture diffusion equation

$$\left[D_m\left(m_{,j}\right)_{,i}\right] + D_m^T\varphi_{,ij} + \frac{E_g N}{\tau K_m} = \left[\frac{\partial m}{\partial t} + \frac{\beta_{ij}^m m_0 D_m \dot{e}_{ij}}{K_m}\right] \tag{2.9}$$

5. Heat conduction equation

$$\left[D_T\left(\varphi_{,j}\right)_{,i}\right] + D_T^m m_{,ij} + \frac{E_g N}{\tau\rho C_E} = \left[\dot{T} + \frac{\beta_{ij}^T T_0}{\rho C_E}\dot{e}_{ij}\right] \tag{2.10}$$

where, $D_{T\rho}C_E = K_{ij} = K_i\delta_{ij}$, i is not summed. The use of a comma after a subscript indicates a partial derivative with respect to space coordinates, while a dot above a variable denotes differentiation with respect to the time variable t.

3. Mathematical model

The semiconductor solid sphere being discussed (Figure 1) exhibits characteristics of axisymmetric, ensuring that it possesses symmetry around its central axis. Additionally, the sphere demonstrates thermal homogeneity, and a radius of r_0 . An external laser pulse heating device has been utilized to effectively heat the outer surface of the sphere. In order to solve the problem at hand, we must take into account the given spherical polar coordinate system (r, θ, φ) with the origin at the center of the sphere and the z-axis as the axis of symmetry. The initial temperatures of the sphere, represented by T_0 , have been kept constant and uniform.

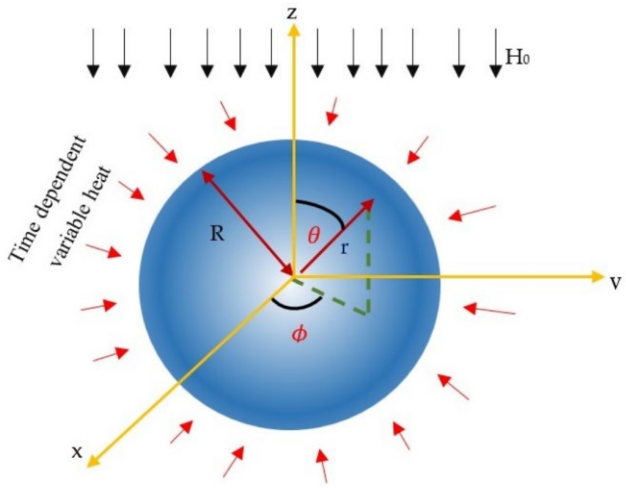

Figure 1: Structure of problem

It is worth noting that, as per the regularity criterion, all fields within a medium are assumed to have finite characteristics. This is an important consideration when examining the functions in question, as their dependence on both radial distance r and time t must be taken into account. This is particularly relevant in the perspective of a 1-D problem where symmetry plays a significant role. Therefore, it is crucial to carefully consider these factors when analyzing the problem at hand. The formulation of the expressions demonstrating the relationships between displacement-strain and components of displacement can be achieved as a result of the given conditions are:

$$\boldsymbol{u} = (u_\rho, u_\theta, u_\phi) = (u, 0, 0)(r, t), \tag{3.1}$$

$$e_{rr} = \frac{\partial u}{\partial r}, \quad e_{\theta\theta} = e_{\phi\phi} = \frac{u}{r}, \quad e_{r\theta} = e_{r\phi} = e_{\theta\phi} = 0. \tag{3.2}$$

The equation (3.1) will take the form when utilizing (2.1) as

$$\sigma_{rr} = (\lambda + 2\mu) + 2\lambda\frac{u}{r} - \left(\beta^T T + \beta^m m + \delta_n N\right), \tag{3.3}$$

$$\sigma_{\theta\theta} = \sigma_{\phi\phi} = \lambda\frac{\partial u}{\partial r} + 2(\lambda + \mu)\frac{u}{r} - \left(\beta^T T + \beta^m m + \delta_n N\right). \tag{3.4}$$

The dilatation term e can be determined by

$$e = \frac{1}{r^2}\frac{\partial(r^2 u)}{\partial r}. \tag{3.5}$$

The equation of motion can be transformed as

$$\frac{\partial \sigma_{rr}}{\partial r} + \frac{1}{r}\left(2\sigma_{rr} - \sigma_{\theta\theta} - \sigma_{\phi\phi}\right) = \rho\frac{\partial^2 u}{\partial t^2}. \tag{3.6}$$

Utilizing equations (3.3)-(3.4), in equations (3.6) yields:

$$(\lambda + 2\mu)\frac{\partial e}{\partial r} - \beta^T\frac{\partial}{\partial r}\left(1 - a\nabla^2\right)\varphi - \beta^m\frac{\partial m}{\partial r} - \delta_n\frac{\partial N}{\partial r} = \rho\left(\frac{\partial^2 u}{\partial t^2}\right). \tag{3.7}$$

The Laplacian operator ∇^2 in the spherical coordinate system, is given by

$$\nabla^2 = \frac{\partial^2}{\partial r^2} + \frac{2}{r}\frac{\partial}{\partial r} = \frac{1}{r^2}\frac{\partial}{\partial r}\left(r^2\frac{\delta}{\delta r}\right). \tag{3.8}$$

Pre-operating both sides of eq (3.7) by $\left(\frac{2}{r} + \frac{\partial}{\partial r}\right)$, yields

$$(\lambda + 2\mu)\nabla^2 e - \beta^T\nabla^2\left(1 - a\nabla^2\right)\varphi - \beta^m\nabla^2 m - \delta_n\nabla^2 N = \left(\frac{\partial^2 e}{\partial t^2}\right). \tag{3.9}$$

Also, equations (3.7), (3.9), and (3.10) can be written as,

$$\frac{\partial N}{\partial t} = \left(D_E\left(\nabla^2 N\right) - \frac{N}{\tau}\right) + k\left(1 - a\nabla^2\right)\varphi, \tag{3.10}$$

$$K_m\left[D_m\nabla^2 m\right] + K_m D_m^T\nabla^2\varphi + \frac{E_g N}{\tau} = \left[K_m\frac{\partial m}{\partial t} + \beta^m m_0 D_m\frac{\partial e}{\partial t}\right], \tag{3.11}$$

$$K\nabla^2\varphi + \rho C_E D_T^m\nabla^2 m + \frac{E_g N}{\tau} = \left[\rho C_E\frac{\partial}{\partial t}\left(1 - a\nabla^2\right)\varphi + \beta^T T_0\frac{\partial e}{\partial t}\right]. \tag{3.12}$$

Pre-operating both sides of eq (3.9) by $\left(\frac{1}{r}+\frac{\partial}{\partial r}\right)$, we obtain

$$(\lambda+2\mu)\nabla^2 e-\beta^T\nabla^2\left(1-a\nabla^2\right)\varphi-\beta^m\nabla^2 m-\delta_n\nabla^2 N=\left(\frac{\partial^2 e}{\partial t^2}\right). \tag{3.13}$$

The equations mentioned above can be converted into dimensionless form using the following subsequent dimensionless quantities.

$$(r',u')=\nu_0\eta(r,u),\quad \left(T',N',\sigma'_{ij},\varphi',m'\right)=\frac{1}{\rho\nu_0^2}\left(\beta^T T,\delta_n N,\sigma_{ij},\varphi,\beta^m m\right),$$

$$\left(\tau'_0,\tau',t'\right)=\nu_0^2\eta(\tau_0,\tau,t),\quad a'=\frac{a}{\eta^2},\quad \eta=\frac{\rho C_E}{K},\quad \rho\nu_0^2=\lambda+2\mu,\quad \gamma=\sqrt{\frac{\mu}{\lambda+2\mu}}. \tag{3.14}$$

After applying the equation (3.14) to equations (3.10)-(3.13) and removing the primes, the resulting equations are obtained as

$$\nabla^2 e-\nabla^2\left(1-a\nabla^2\right)\varphi-\nabla^2 m-\left(\nabla^2 N\right)=\left(\frac{\partial^2 e}{\partial t^2}\right), \tag{3.15}$$

$$\frac{\partial N}{\partial t}=\left(\delta_1(\nabla^2 N)-\delta_2 N\right)+\delta_3\left(1-a\nabla^2\right)\varphi, \tag{3.16}$$

$$\left[\nabla^2 m\right]+\delta_8\nabla^2\varphi+\delta_9\frac{\partial N}{\partial t}=\left[\delta_{10}\frac{\partial m}{\partial t}+\delta_{11}\frac{\partial e}{\partial t}\right], \tag{3.17}$$

$$\nabla^2\varphi+\delta_{12}\nabla^2 m+\delta_5 N=\left[\delta_{13}\frac{\partial}{\partial t}\left(1-a\nabla^2\right)\varphi+\delta_6\frac{\partial e}{\partial t}\right], \tag{3.18}$$

where

$$\delta_1=D_E\eta,\quad \delta_2=\frac{1}{\tau},\quad \delta_3=\frac{k\delta_n}{\beta^T},\quad \delta_5=\frac{\beta^T E_g}{\delta_n C_E(\lambda+2\mu)\eta\tau},\quad \delta_6=\frac{\left(B^T\right)^2 T_0}{\rho C_E(\lambda+2m)},\quad \delta_8=\frac{\beta^m D_m^T}{v_0^2\eta D_m},$$
$$\delta_9=\frac{E_g\beta^m}{\tau v_0^2\eta^2\delta_n K_m D_m},\quad \delta_{10}=\frac{1}{\eta D_m},\quad \delta_{11}=\frac{(\beta^m)^2 m+0}{\rho v_0^2\eta K_m},\quad \delta_{12}=\frac{\beta^T D_T^m}{v_0^4\eta^2},\quad \delta_{13}=\frac{\beta^T}{(\lambda+2\mu)}.$$

After applying the equation (3.14) to equations (3.3)-(3.4) and removing the primes, the resulting equations are obtained as

$$\sigma_{rr} = \gamma^2 \frac{\partial u}{\partial r} + (1-\gamma^2)e - \left((1-a\nabla^2)\,\varphi + m + N\right), \tag{3.19}$$

$$\sigma_{\theta\theta} = \sigma_{\phi\phi} = \gamma^2 \frac{u}{r} + (1-\gamma^2)e - \left((1-a\nabla^2)\,\varphi + m + N\right). \tag{3.20}$$

Initial conditions are assumed as

$$u(r,0) = 0 = \frac{\partial u}{\partial r}(r,0), \tag{3.21}$$

$$T(r,0) = 0 = \frac{\partial T}{\partial r}(r,0), \tag{3.22}$$

$$N(r,0) = 0 = \frac{\partial N}{\partial r}(r,0), \tag{3.23}$$

$$m(r,0) = 0 = \frac{\partial m}{\partial r}(r,0). \tag{3.24}$$

The Laplace transform of a function f w.r.t. time variable t, is defined as

$$\mathcal{L}\left(f(t)\right) = \bar{f}(s) = \int_0^\infty f(t)e^{-st}dt. \tag{3.25}$$

Using Laplace transforms from eq. (3.25) to (3.15)-(3.18) yields

$$\left(\nabla^2 - s^2\right)\bar{e} - \nabla^2\left(1-a\nabla^2\right)\bar{\varphi} - \nabla^2\bar{m} - \nabla^2\bar{N} = 0, \tag{3.26}$$

$$(\delta_1\nabla^2 - \delta_{14})\bar{N} + \delta_3\left(1-a\nabla^2\right)\bar{\varphi} = 0, \tag{3.27}$$

$$\delta_{18}\bar{e} + \left(\nabla^2 + \delta_{20}\right)\bar{m} + \delta_8\nabla^2 \bar{varphi} + \delta_9 s\bar{N} = 0, \tag{3.28}$$

$$\delta_{15}\bar{e} + \left(\delta_{17}\nabla^2 + \delta_{16}\right)\bar{varphi} + \delta_5\bar{N} + \delta_{12}\nabla^2\bar{m} = 0, \tag{3.29}$$

where

$$\delta_{14} = \delta_2 + s, \quad \delta_{15} = -\delta_6 s, \quad \delta_{16} = -\delta_{13}s, \quad \delta_{17} = (1 + a\delta_{13}s), \quad \delta_{18} = -\delta_{11}s, \quad \delta_{20} = -\delta_{10}s.$$

Utilizing equation (3.25) to equations (3.19)-(3.20), yields

$$\overline{\sigma_{rr}} = \gamma^2 \frac{\partial \bar{u}}{\partial r} + (1-\gamma^2)\bar{e} - \left((1-a^2\nabla^2)\bar{\varphi} + \bar{m} + \bar{N}\right), \tag{3.30}$$

$$\overline{\sigma_{\theta\theta}} = \gamma^2 \frac{\bar{u}}{r} + (1-\gamma^2)\bar{e} - \left((1-a^2\nabla^2)\bar{\varphi} + \bar{m} + \bar{N}\right). \tag{3.31}$$

When Eqs. (3.26) to (3.29) are decoupled, we get

$$\left(\nabla^8 + B\nabla^6 + C\nabla^4 + D\nabla^2 + E\right)(\bar{e}, \bar{\varphi}, \bar{m}, \bar{N}), \tag{3.32}$$

where

$$\begin{aligned}
A &= -\delta_1\delta_8\delta_{12} + \delta_1\delta_{17} + a\delta_1\delta_{18}\delta_{12} - a\delta_1\delta_{15},\\
B &= (a\delta_3(\delta_5 - s\delta_9\delta_{12} - \delta_{18}\delta_{12} + \delta_{15}) + \delta_{14}\delta_8\delta_{12} - \delta_{14}\delta_{17} + \delta_8\delta_{12}\delta_{14} - \delta_{15}\delta_{14}\\
&\quad - \delta_1(-\delta_{16} - \delta_{17}\delta_{20} + (-\delta_8\delta_{12} + \delta_{17})s^2 - \delta_{15} + \delta_{18}\delta_{12} + a\delta_{15}\delta_{20} - \delta_{18}\delta_{17} + \delta_{15}\delta_8))/A,\\
C &= (-\delta_3(\delta_5 - s\delta_9\delta_{12} - \delta_{18}\delta_{12} + \delta_{15}) + a\delta_3(\delta_{20}\delta_5 - s^2\delta_5 + \delta_{12}\delta_9 s^3 - \delta_9\delta_{15}s + \delta_{18}\delta_5 - \delta_{15}\delta_{20})\\
&\quad + \delta_{14}(\delta_{18}\delta_{12} - \delta_{16} - \delta_{17}\delta_{20} - (\delta_{12}\delta_8 - \delta_{17})s^2 - \delta_{15} + a\delta_{15}\delta_{20} - \delta_{18}\delta_{17} + \delta_{15}\delta_8)\\
&\quad - \delta_1(-\delta_{16}\delta_{20} - s^2(-\delta_{16} - \delta_{17}\delta_{20}) - \delta_{15}\delta_{20}))/A\\
D &= (-a\delta_3\delta_{20}\delta_5 s^2 - \delta_3(\delta_{20}\delta_5 - s^2\delta_5 + \delta_{12}\delta_9 s^3 - \delta_9\delta_{15}s + \delta_{18}\delta_5 + \delta_{15}\delta_{20})\\
&\quad + \delta_{14}(-\delta_{16}\delta_{20} - s^2(-\delta_{16} - \delta_{17}\delta_{20}) - \delta_{15}\delta_{20}) - \delta_1\delta_{16}\delta_{20}s^2)/A,\\
E &= \left(\delta_{14}\delta_{16}\delta_{20}s^2 + \delta_3\delta_{20}\delta_5 s^2\right)/A.
\end{aligned}$$

Let λ_i, $i = 1, 2, 3, 4$ be the roots of equation (2.32), so we can write

$$(\nabla^2 - \lambda_1^2)(\nabla^2 - \lambda_2^2)(\nabla^3 - \lambda_3^2)(\nabla^2 - \lambda_4^2)(\bar{e}, \bar{\varphi}, \bar{m}, \bar{N}) = 0 \tag{3.33}$$

where λ_i^2, $i = 1, 2, 3, 4$ are the roots of the characteristic equation of equation (3.32)

$$\lambda^8 + B\lambda^6 + C\lambda^4 + D\lambda^2 + E = 0. \tag{3.34}$$

The general solution of Eq. (2.33) can be written in the form

$$(\bar{e}, \bar{\varphi}, \bar{m}, \bar{N}) = \sum_{i=1}^{4} (1, \zeta_i, \eta_i, \omega_i)\, g_i I_{1/2}(\lambda_i r), \tag{3.35}$$

where $I_n()$ specifies the modified Bessel functions of second types of order n. The relation for Bessel function is

$$\int x^{3/2} I_{1/2}(x)dx = x^{3/2} I_{3/2}(x). \tag{3.36}$$

By introducing Eq. (3.35) into Eqs. (3.26)–(3.29), we obtain the following expression

$$\zeta_i = \frac{(\lambda_i - s^2)\left[(\lambda_i^2+\delta_{20})\delta_5 - \delta_9\delta_{12}s\lambda_i^2\right] + \lambda_i^2(\delta_5\delta_{18}s - \delta_{15}\delta_9 s) - \lambda_i^2\left[\delta_{18}\delta_{12}\lambda_i^2 - \delta_{15}(\delta_{19}\lambda_i^2+\delta_{20})\right]}{\left(\delta_3(1-a\lambda_i^2)\right)\left[\delta_5\lambda_i^2+\delta_5\delta_{20}-\delta_9\delta_{12}s\lambda_i^2\right] + (\delta_1\lambda_i^2-\delta_{14})s^2\left[\delta_8\delta_{12}\lambda_i^4 - (\lambda_i^2+\delta_{20})(\delta_{17}\lambda_i^2+\delta_{16})\right]}, \tag{3.37}$$

$$\eta_i = \frac{(\lambda_i^2 - s^2)\left[\delta_5\delta_3\left(1-a\lambda_i^2\right) - \left(\delta_{17}\lambda_i^2+\delta_{16}\right)\left(\delta_1\lambda_i^2-\delta_{14}\right)\right] - \delta_{15}\left(1-\lambda_i^2\right)\lambda_i^2\left[-\left(\delta_1\lambda_i^2-\delta_{14}\right)+\right.}{\left(\delta_3(1-a\lambda_i^2)\right)\left[\delta_5\lambda_i^2+\delta_5\delta_{20}-\delta_9\delta_{12}s\lambda_i^2\right] + (\delta_1\lambda_i^2-\delta_{14})s^2\left(\delta_8\delta_{12}\lambda_i^4 - (\lambda_i^2+\delta_{20})(\delta_{17}\lambda_i^2+\delta_1\right.} \tag{3.38}$$

$$\omega_i = \frac{\left(\delta_3(1-a\lambda^{-2})\right)\left[(\lambda_i^2-s^2)(\lambda_i^2+\delta_{20}+\delta_{18}\lambda_i^2\right]}{\left(\delta_3(1-a\lambda_i^2)\right)\left[\delta_5\lambda_i^2+\delta_5\delta_{20}-\delta_9\delta 12s\lambda_i^2\right] + (\delta_1\lambda_1^2-\delta_{14})s^2\left(\delta_8\delta_{12}\lambda_i^4 - (\lambda_i^2+\delta_{20})(\delta_{17}\lambda_i^2+\delta_{16})\right)}. \tag{3.39}$$

The expression for the displacement u in the Laplace transforms domain is as follows:

$$\bar{u} = \frac{1}{\sqrt{r}}\sum_{i=1}^{4}\frac{1}{\lambda_i} g_i I_{3/2}(\lambda_i r). \tag{3.40}$$

The modified Bessel I_n is defined by the following relationships for any positive number x.

$$I_{1/2} = \sqrt{\frac{2}{\pi x}}\sinh x, \tag{3.41}$$

$$I_{3/2} = \sqrt{\frac{2}{\pi x}}\left(\cosh x - \frac{\sinh x}{x}\right). \tag{3.42}$$

By utilizing Eq. (3.41) into Eqs. (3.35), yields

$$\left(\bar{e}, \bar{\varphi}, \bar{m}, \bar{N}\right) = \sqrt{\frac{2}{\pi}}\sum_{i=1}^{4}\left(1, \zeta_i, \eta_i, \omega_i\right)\frac{g_i}{\sqrt{r\lambda_i}}\sinh(\lambda_i r). \tag{3.43}$$

The displacement $\bar{u}$ can be expressed in the Laplace transform domain by utilizing equation (3.25) in (3.40) as

$$\bar{u} = \sqrt{\frac{2}{\pi}}\sum_{i=1}^{4}\frac{g_i}{\lambda_i^{3/2}}\left(\cosh(\lambda_i r) - \frac{\sinh(\lambda_i r)}{(\lambda_i r)}\right). \tag{3.44}$$

Differentiating equation (3.40) in terms of r yields

$$\frac{\partial \bar{u}}{\partial r} = \sqrt{\frac{2}{\pi}} \sum_{i=1}^{4} g_i \{ l_i \sinh(\lambda_i r) - n_i \cosh(\lambda_i r) \}, \tag{3.45}$$

$$l_i = \left(\frac{2 + \lambda_i^2 r^2}{r^3 \lambda_i^{5/2}} \right), \quad n_i = \frac{2}{r^2 \lambda_i^{3/2}}.$$

Thus, using (3.43)-(3.45) in equations (3.30) and (3.31), the expressions for thermal stresses are derived as

$$\overline{\sigma_{rr}} = \sqrt{\frac{2}{\pi}} \sum_{i=1}^{4} g_i \{ l1_i \sinh(\lambda_i r) - n1_i \cosh(\lambda_i r) \}, \tag{3.46}$$

$$\overline{\sigma_{\theta\theta}} = \sqrt{\frac{2}{\pi}} \sum_{i=1}^{4} g_i \{ p_i \cosh(\lambda_i r) - m_i \sinh(\lambda_i r) \}, \tag{3.47}$$

$$p_i = \frac{\gamma^2}{r^2 \lambda_i^{3/2}}, \quad m_i = \left(\frac{-\gamma^2}{r^{5/2} \lambda_i^2} \right) + \frac{1 - \gamma^2 - (\zeta_i + \eta_i)}{r^{1/2} \lambda_i^{1/2}}, \tag{3.48}$$

$$l1_i = \left(\gamma^2 l_i + \frac{1 - \gamma^2 - (\zeta_i + \eta_i)}{r^{1/2} \lambda_i^{1/2}} \right), \quad n1_i = \gamma^2 n_i. \tag{3.49}$$

4. Boundary conditions

The mechanical boundary condition can be expressed as the exterior surface of the sphere being traction-free and constrained by a time-dependent variable heat

$$T(R,t) = T_1 H(t), \; t > 0, \tag{4.1}$$

$$\sigma_{rr}(R,t) = 0. \tag{4.2}$$

In the diffusion phase, carriers have the possibility of reaching the surface of the sphere and may recombine with a finite probability. As a result, the boundary condition for carrier density is established as

$$D_E \frac{\partial N}{\partial r} = S_v N, \quad \text{at} \quad r = R. \tag{4.3}$$

The following moisture diffusion boundary condition is applied at the boundary surface when $r = r_0$

$$m = 0 \text{ at } r = r_0. \tag{4.4}$$

By applying the Laplace transform on (4.1)-(4.4) yields

$$\left(1 - a\nabla^2\right)\bar{\varphi}(R,s) = \frac{T_0}{s}, \tag{4.5}$$

$$\bar{\sigma}_{rr}(R,s) = 0, \tag{4.6}$$

$$D_E \left.\frac{\partial \bar{N}}{\partial r}\right|_{r=r_0} = s_v \bar{N}(R,s), \tag{4.7}$$

$$\bar{m} = 0 \quad \text{at} \quad r = R. \tag{4.8}$$

Equations (3.39) and (3.36) are substituted into Eq. (4.5)-(4.8), giving

$$\sqrt{\frac{2}{\pi}} \sum_{i=1}^{4} g_i \left\{ \left(1 - a\lambda_i^2\right) \frac{\zeta_i}{\sqrt{\lambda_i R}} \sinh(\lambda_i R) \right\} = \frac{T_0}{s}, \tag{4.9}$$

$$\sum_{i=1}^{4} g_i \left\{ \, l1_i \sinh(\lambda_i R) - n1_i \cosh(\lambda_i R) \right\} = 0, \tag{4.10}$$

$$\sum_{i=1}^{4} g_i \eta_i \left\{ \, a_i \cosh(\lambda_i R) + b_i \sinh(\lambda_i R) \right\} = 0, \tag{4.11}$$

$$\sqrt{\frac{2}{\pi}} \sum_{i=1}^{4} \eta_i \frac{g_i}{\sqrt{R\lambda_i}} \sinh(\lambda_i R) = 0, \tag{4.12}$$

$$a_i = \frac{D_E \lambda_i^{1/2}}{R^{1/2}}, \quad b_i = \frac{-D_E}{2R^{3/2}\lambda_i^{3/2}} - \frac{s_v}{\sqrt{\lambda_i R}},$$

$$n_{1i} = \left(\gamma^2 l_{1i} + \frac{1 - \gamma^2 - (\zeta_i + \eta_i)}{R\lambda_i^{1/2}} \right), \quad l_{1i} = \left(\frac{2 + \lambda_i^2 R^2}{R^3 \lambda_i^{5/2}} \right).$$

The values of g_i, $i = 1, 2, 3, 4$ can be obtained by solving equations (4.9)-(4.12) by Cramer's rule

$$g_i(s) = \frac{\Delta_i}{\Delta}, \tag{4.13}$$

$$\Delta = \begin{bmatrix} G_{11} & G_{12} & G_{13} & G_{14} \\ G_{21} & G_{22} & G_{23} & G_{24} \\ G_{31} & G_{32} & G_{33} & G_{34} \\ G_{41} & G_{42} & G_{43} & G_{44} \end{bmatrix}. \tag{4.14}$$

Δ_i is obtained from Δ by replacing its i^{th} column by $\begin{bmatrix} \frac{T_0}{s} & 0 & 0 & 0 \end{bmatrix}$. (4.15)

$$\begin{aligned} G_{1i} &= \sqrt{\frac{2}{\pi}} \left\{ \frac{\zeta_i}{\sqrt{\lambda_i R}} (1 - a\lambda_i^2) \right\}, \\ G_{2i} &= \{ l1_i \sinh(\lambda_i R) - n1_i \cosh(\lambda_i R) \}, \\ G_{3i} &= \eta_i \{ a_i \cosh(\lambda_i R) + b_i \sinh(\lambda_i R) \}, \\ G_{4,i} &= \sqrt{\frac{2}{\pi}} \frac{\eta_i}{\sqrt{R\lambda_i}} \sinh(\lambda_i R), \\ i &= 1, 2, 3, 4. \end{aligned}$$

Using the values of $g_i(s)$ from (4.13) in (3.43), (3.44), and (3.46)-(3.47) the expression for displacement, carrier density, stresses, and temperature distribution can be obtained.

5. Inversion of the transforms

To obtain the solution in the physical domain, the transforms in equations (3.49) and (4.4) need to be inverted by using

$$f(x,t) = \frac{1}{2\pi i} \int_{e^{-i\infty}}^{+i\infty} \tilde{f}(x,s) e^{-st} ds. \tag{5.1}$$

To evaluate the integral in equation (5.1), it is recommended to apply Romberg's integration [27] with an adaptive step size. This method involves dividing the integration interval into smaller subintervals and approximating the integral using a combination of these subintervals. The adaptive step size ensures that the approximation is accurate and efficient, as it adjusts the size of the subintervals based on the function's behavior. By using this method, the integral can be evaluated with

6. Numerical results and discutions

The physical data of silicon (Si) material is utilized in this study to show the theoretical findings and visually represent the impact of two temperatures using MATLAB software.

$\lambda = 3.64 \times 10^{10} Nm^{-2}$, $T_0 = 300$ K,
$\mu = 5.46 \times 10^{10} Nm^{-2}$, $H_0 = 1 Jm^{-1} nb^{-1}$,
β=7.04 $\times \times 10^{6}$ Nm^{-2} deg^{-1}, $\tau = 5 \times 10^{-5}$ s,
δ_n = -9 $\times 10^{-31} m^{-3}$, $N_0 = 10^{20} m^{-3}$,
$\rho = 2.33 \times 10^{3} Kgm^{-3}$, $\varepsilon_0 = 8.838 \times 10^{-12} Fm^{-1}$,
$C_E = 695 JKg^{-1} K^{-1}$, $E_g = 1.11$ e V,
$K = 150 Wm^{-1} K^{-1}$, $\alpha_T = 3 \times 10^{-6} K^{-1}$,
$K^* = 1.54 \times 10^{2} Ws$, $s_v = 2ms^{-1}$,
$D_E = 2.5 \times 10^{-3} m^2 s^{-1}$, $H_0 = 10^{8} Col.cm^{-1} s^{-1}$,
$\mu_0 = 4\pi \times 10^{-7} Hm^{-1}$. $\sigma_0 = 9.36 \times 10^{5} Col^2 C^{-1} m^{-1} s^{-1}$.

The data presented in the figures pertains to four distinct cases of the two temperatures parameter. These cases are represented by solid black lines (a = 0.02), solid red lines (a = 0.04), solid blue lines (a = 0.06), and solid purple lines (a = 0.08). The analysis of these cases is based on the temperature parameter, which is a crucial factor in determining the behavior of the system under consideration. The radial displacement u for the hygro- photo-thermoelasticity model with two temperatures parameter is illustrated in Figure 2, exhibiting a distinct pattern. Initially, the displacement starts from a positive zero value and experiences a rapid surge, eventually reaching a peak maximum value near r = 0.7. This behavior can be attributed to the combined effects of photo-excitation and moisture diffusivity. Notably, as the two temperatures parameter increases, there is a noticeable increase in the radial displacement. This observation suggests a correlation between the two temperatures parameter and the magnitude of radial displacement, indicating that higher values of the two temperatures parameter result in higher value of displacement. For the parameter value a = 0.02 of the two temperatures parameter, the radial displacement exhibits the lowest deviation.

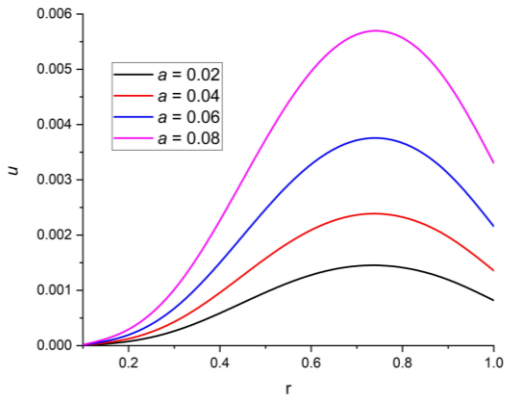

Figure 2: The radial displacement variation with two temperatures

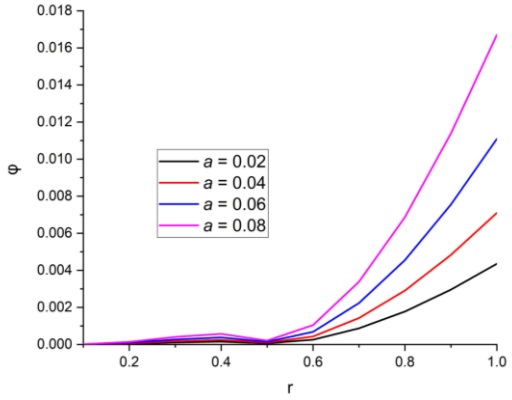

Figure 3: The variation in temperature distribution with two temperatures

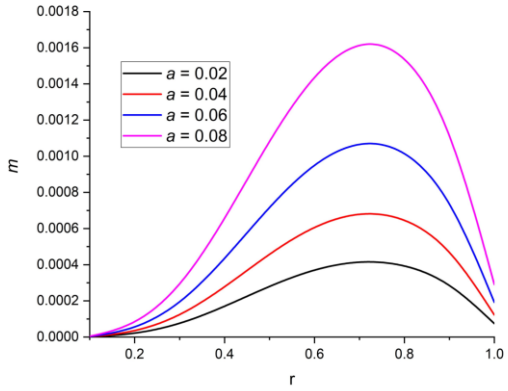

Figure 4: The moisture diffusion variation with two temperatures

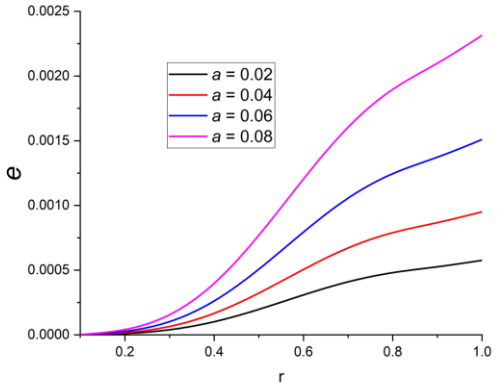

Figure 5: The variation in dilatation distributions with two temperatures

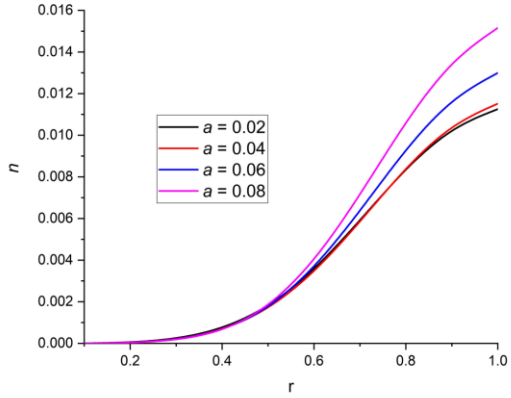

Figure 6: The deviation in carrier density with two temperatures

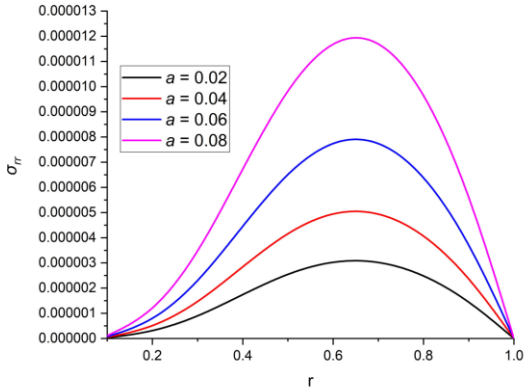

Figure 7: The deviation in radial stress with two temperatures

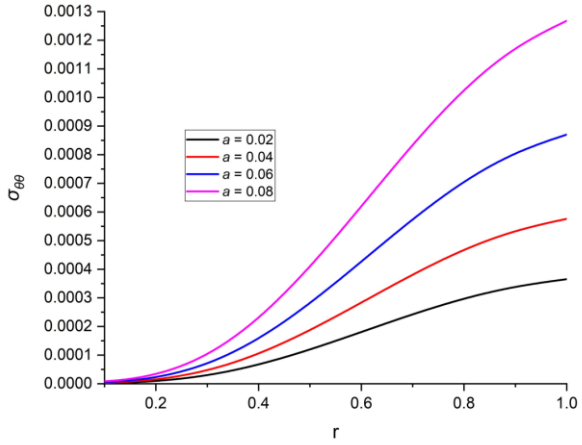

Figure 8: The deviation in hoop stress with two temperatures

The moisture diffusion behavior of the hygro- photo-thermoelasticity model is depicted in Figure 4, considering different values of two temperatures parameter.
It is noteworthy that a higher value of this parameter leads to increased variability in moisture diffusion, while a lower value results in reduced variability. In each of the four situations corresponding to the two temperatures parameter, the moisture diffusion initiates from zero and attains maximum values near the surface. Additionally, it is important to mention that at **r=0** and **r=R**, the moisture diffusion complies with the boundary condition specified in equation (2.8) by being zero.
Figure 5 displays the dilatation distributions for the hygro- photo-thermoelasticity model at various values of two temperatures parameter. The results indicate that lower values of the two temperatures parameter exhibit greater variability in dilatation distributions compared to higher values. Additionally, as the radial distance r increases, the variability in dilatation distributions is observed to significantly in- crease. These findings suggest that the two temperatures parameter plays a crucial role in determining the dilatation distributions of the hygro-photo-thermoelasticity model, and that the radial distance r should also be taken into account when analyzing these distributions. In each of the four situations corresponding to the two temperatures parameter, the dilatation initiates from zero and attains maximum values near the surface. The fluctuation in carrier density for the hygro-photo-thermoelasticity model at various temperatures is illustrated in Figure 6. It is observed that an increase in temperature values leads to an increase in carrier density.
Additionally, it is noted that as the radial distance r expands, there is a significant increase in the variance of carrier density. In all four situations corresponding to the temperature parameter, the carrier density starts from zero and reaches maximum values near the surface. This behavior can be attributed to the combined effects of photo-excitation and moisture diffusivity.
Figures 7 to 8 illustrate the changes in stress components for the hygro-photo-thermoelasticity model when considering the two temperatures parameter. It is evident that there is an upward trend in the stress components as the values of the two temperatures parameter increase. In all four scenarios associated with the two temperatures parameter, the σ_{rr} starts from zero and reaches its peak values near the surface. It is worth mentioning that at **r=0** and **r=R**, the σrr adheres to the boundary condition specified in equation (2.6) by being zero. Moreover, in each of the four situations corresponding to the two temperatures parameter, the $\sigma_{\theta\theta}$ begins from zero and attains its maximum values near the surface.

7. Conclusions

In this study, a unique methodology is employed to explore the influence of photothermoelasticity theory on moisture diffusivity in an elastic semiconductor sphere. The primary objective of this study is to analyze the effects of applying an exponential laser pulse on the surface of an infinite semiconducting solid sphere.

The governing equations are derived for hygro- photo-thermoelasticity with two temperatures, incorporating both thermal and moisture diffusivity.

- The study presents graphical illustrations that effectively depict the influence of two temperatures parameter on multiple components, including displacement, thermal stresses, dilation distributions, moisture diffusivity, carrier density, and temperature field. Through these visual representations, it becomes evident that the factors associated with the two temperatures parameter hold substantial importance in the domains under investigation. The graphs provide a comprehensive understanding of the impact of these parameters on the various components, thereby contributing to the overall comprehension of the subject matter.
- The thermal effect arises when semiconductor materials are exposed to concentrated laser beams or beams of sunlight. These materials find wide-ranging applications in the renewable energy sector, with a particular emphasis on the solar cell industry, where semiconductor materials play a crucial role.
- The semiconductor sphere with two temperature is an innovative and promising technology that has the potential to revolutionize the field of thermoelectrics. This concept involves utilizing hyperbolic materials with unique energy transfer properties to create a thermal diode effect, enabling efficient conversion of heat into electricity. By maintaining a temperature gradient across the semiconductor sphere, the device can harvest waste heat or solar radiation and convert it into usable electrical power. The two temperature approach enhances the efficiency of this process by effectively managing the temperature distribution within the material. This technology holds great promise for various applications, such as waste heat recovery in industrial processes, solar energy harvesting, and even powering electronic devices. Through further research and development, the semiconductor sphere with two temperature could contribute to a more sustainable and clean energy future.

Competing interests

The authors declare that they have no conflict of interest.

Funding

No fund /grant / scholarship has been taken for the research work

Authors' contributions

Eduard-Marius Craciun: Idea formulation, Formulated strategies for mathematical modelling, methodology refinement, Formal analysis, Validation, Writing- review & editing.

Iqbal Kaur: Idea formulation, Conceptualization, Formulated strategies for mathematical modelling, methodology refinement, Formal analysis, Validation, Writingreview & editing.

Kulvinder Singh: Conceptualization, Effective literature review, Experiments and Simulation, Investigation, Methodology, Software, Supervision, Validation, Visualization, Writing - original draft.

All authors read and approved the final manuscript.

Acknow ledgements

Not applicable

REFERENCES

[1] J.M. Duhamel, Mummy Div. Sav. (AcadSci Par.). 5 (1938) 440-498.
[2] M.A. Biot, J. Appl. Phys. 27 (1956) 240-253.
[3] A. Szekeres, Comput. Struct. 76 (2000) 145-152.
[4] A. Szekeres, J. Therm. Stress. 35 (2012) 248-268.
[5] A. Szekeres, J. Engelbrecht, Period. Polytech. Mech. Eng. 44 (2000) 161-170.
[6] C. Cattaneo, Comptes Rendus, Acad. Sci. Paris, Ser. II. 247 (1958) 431-433.
[7] P. Vernotte, Comptes Rendus, Acad. Sci. Paris, Ser. II. 246 (1958) 3154-3155.
[8] P. Vernotte, Comptes Rendus, Acad. Sci. Paris, Ser. II. 252 (1961) 2190-2191.
[9] H.W. Lord, Y. Shulman, J. Mech. Phys. Solids. 15 (1967) 299-309.
[10] A.E. Green, K.A. Lindsay, J. Elast. 2 (1972) 1-7.
[11] R.S. Dhaliwal, H.H. Sheriff, Q. Appl. Math. 38 (1980) 1-8.
[12] A.E. Green, P.M. Naghdi, Proc. R. Soc. London. Ser. A Math. Phys. Sci. 432 (1991) 171-194.
[13] A.E. Green, P.M. Naghdi, J. Therm. Stress. 15 (1992) 253-264.
[14] A.E. Green, P.M. Naghdi, J. Elast. 31 (1993) 189-208.
[15] J.R. Fernandez, R. Quintanilla, Appl. Math. Mech. 2021 422. 42 (2021) 309-316.
[16] I. Kaur, K. Singh, E.-M. Craciun, Mathematics. 10 (2022) 2386.
[17] I. Kaur, K. Singh, Partial Differ. Equations Appl. Math. 4 (2021) 100130.
[18] I. Kaur, K. Singh, Int. J. Mech. Mater. Eng. 16 (2021) 1-16.
[19] X.-Y. Zhang, X.-F. Li, Thin-Walled Struct. 168 (2021) 108283.
[20] J.S. Mohamed Ali, S. Alsubari, Y. Aminanda, Lat. Am. J. Solids Struct. 13 (2016) 573-589.
[21] I. Kaur, P. Lata, K. Singh, Arch. Appl. Mech. 91 (2021) 317-341.
[22] I. Kaur, K. Singh, E.-M. Craciun, Discov. Mech. Eng. 2 (2023) 2.
[23] I. Kaur, K. Singh, E.-M. Craciun, Mathematics. 11 (2023) 432.
[24] F. Ebrahimi, A. Dabbagh, F. Tornabene, O. Civalek, Adv. Nano Res. 7 (2019) 157-166.
[25] I. Kaur, P. Lata, Int. J. Mech. Mater. Eng. 15 (2020).
[26] K. Singh, I. Kaur, E.-M. Craciun, Mathematics. 11 (2023) 1-13.
[27] William H. Press, Saul A. Teukolsky, Brian P. Flannery, Cambridge University Press, Cambridge, 1980.